

Electrostatic Membrane Deformable Mirror Characterization and Applications

Keith Bush, Anthony Marrs, Michael Schoen

AgilOptics, Inc.

1717 Louisiana, NE Suite 202, Albuquerque, NM 87110

kbush@agiloptics.com

ABSTRACT

Electrostatic Membrane Deformable Mirror (MDM) technology developed using silicon bulk micro-machining techniques offers the potential of providing low-cost, compact wavefront control systems for diverse optical system applications. Electrostatic mirror construction using bulk micro-machining allows for custom designs to satisfy wavefront control requirements for most optical systems. An electrostatic MDM consists of a thin membrane, generally with a thin metal or multi-layer high-reflectivity coating, suspended over an actuator pad array that is connected to a high-voltage driver. Voltages applied to the array elements deflect the membrane to provide an optical surface capable of correcting for measured optical aberrations in a given system. Electrostatic membrane DM designs are derived from well-known principles of membrane mechanics and electrostatics, the desired optical wavefront control requirements, and the current limitations of mirror fabrication and actuator drive electronics. MDM performance is strongly dependent on mirror diameter and air damping in meeting desired spatial and temporal frequency requirements. In this paper, we discuss characterization measurements and modeling of MDM spatial and temporal performance for different mirror designs and present application results illustrating the diverse uses of MDM technology in optical wavefront compensation systems.

Keywords: deformable mirror, electrostatic, membrane, wavefront control, MEMS applications

1.0 INTRODUCTION

The concept of forming a Deformable Mirror (DM) based on electrostatic deflection of a thin membrane was first introduced in the literature in the mid-1970s.¹⁻³ Basic theory and design considerations for developing easily manufactured and inexpensive membrane mirrors from titanium and nickel membrane materials was established. Experimental testing of these devices showed that membrane mirror performance was “predictable and desirable.” Silicon micro-machining has revived the membrane DM concept to produce light-weight, low cost electrostatic membrane mirrors, for many different applications.⁴⁻¹⁰ AgilOptics, Inc. (formerly Intellite, Inc.) has been developing electrostatic Micro-Electromechanical Systems (MEMS) DM technology since 2001 for both commercial and government applications. Our goal is to develop complete low-cost Adaptive Optic (AO) systems including standard and custom MDM designs, driver and control electronics, and open and closed-loop control software. Much of our current research is focused on improving MDM design and fabrication approaches to provide optimum mirror performance for a variety of applications. Better understanding of fabricated MDM designs is obtained through modeling, characterization testing, and application demonstrations. Characterization tests have been performed to evaluate both spatial and temporal performance. Static measurements and modeling indicate that MDMs are capable of large throw, but aberration magnitude correction is spatially dependent. Temporal performance measurements show that MDM throw is quickly reduced by air damping with increasing driving frequency. Throw at higher frequencies is greatly improved with vacuum operation, but is limited, severely in some cases, by low resonance frequencies at large-amplitude driving signals. With actuator-pad air venting, we have been able to obtain a membrane throw in air of greater than 0.7 microns at 1 KHz using a large-amplitude driving signal. We have demonstrated a number of applications using AgilOptics MDM systems. These applications include optical fiber energy optimization, laser beam shaping, laser beam quality improvement, capabilities for high-power wavefront compensation, and aero-optics turbulence compensation. We describe the MDM systems available from AgilOptics for adaptive optics applications in general and provide experiment details and results for these application demonstrations. The aero-optics turbulence compensation results, in particular, illustrate the potential of MDM systems to satisfy requirements for light-weight, low-power, easily deployable, and effective adaptive optics systems.

The technical content of this paper is organized into 5 Sections. Section 2.0 summarizes AgilOptics' electrostatic MDM construction. Electrostatic MDM theory is briefly reviewed in Section 3.0. AgilOptics' MDM systems are discussed in Section 4.0. Section 5.0 provides results from our MDM characterization efforts. MDM application details and results are presented in Section 6.0.

2.0 ELECTROSTATIC MEMBRANE DM CONSTRUCTION

Electrostatic Membrane Deformable Mirrors developed by AgilOptics are fabricated in clean room facilities at the University of New Mexico. Basic MDM construction is illustrated in Figure 1. The mirror membrane is formed by etching away silicon from a masked region on a 1 mm thick silicon wafer previously coated with a silicon-nitride layer. Reflective and conductive coatings are then deposited on the membrane, as necessary, to provide high optical reflectivity and membrane conductivity for actuation. An actuator pad array and conductive leads are patterned and evaporated in gold on a separate silicon wafer. The membrane and pad array wafers are then bonded together with a conductive fixed-size spacer to form the completed mirror. The mirror is actuated by applying voltage to the pad-array actuators or by applying voltage to the membrane conductive surface. The potential difference between these surfaces induces an electrostatic force that causes the membrane to deform in the regions where the difference exists. If excessive voltage is applied, the electrostatic force will overcome the membrane tensile force and the membrane will “snap-down” to the pad array. Without AgilOptics' patent-pending Anti-Snap-Down (ASD) technology the membrane would be destroyed under these conditions. ASD allows for electrostatic snap-down to occur without membrane destruction. Of course, the electrostatic snap-down limit should be avoided for normal mirror operation.

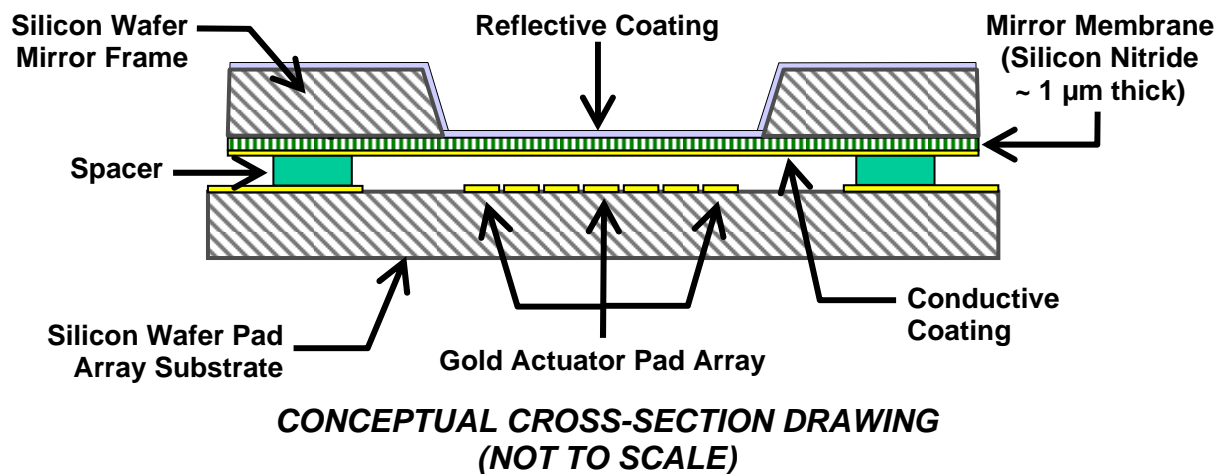
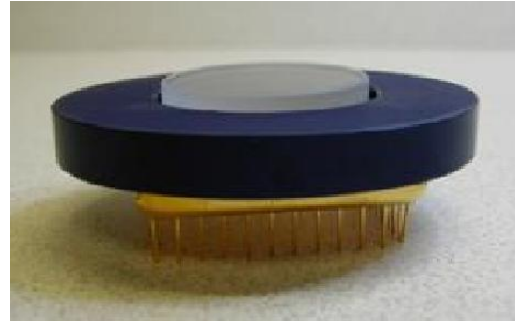
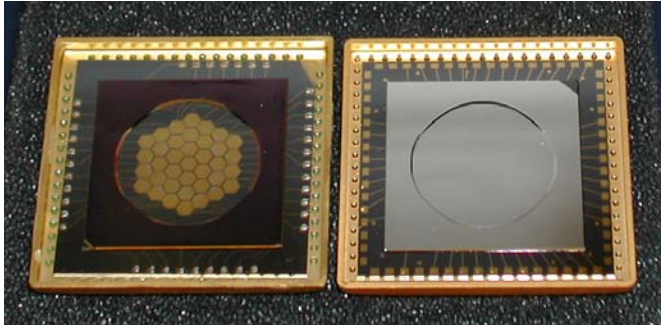


Figure 1. Electrostatic Membrane Deformable Mirror (MDM) construction

AgilOptics develops and markets membrane deformable mirrors and mirror drivers in standard and custom configurations. Some of our standard commercial products are pictured with summarized specifications in Figure 2. Desired High Reflectivity (HR) or standard Aluminum (Al) mirror coatings are available. High voltage electronics designs have been developed to drive up to 1024 channels (SX). In current configurations, these drivers operate through the PC parallel port to drive up to 40 channels. The electronics bandwidth is 30 KHz for the DI model and 2 KHz for the SX model. Despite the high frequency operation of the drivers, the mirror update-rate in this configuration is limited by the PC-Parallel-Port to about 500 Hz.

AgilOptics' latest electronics design and packaging can accommodate up to a 50 mm diameter MDM and apply up to 300 Volts to control each actuator channel. The combination mirror and driver system is known as the “Unifi system” and is pictured in Figure 3 along with some pertinent physical and technical specifications. In the current 64-channel configuration the electronics can update mirror voltages at up to 4 KHz with USB 2.0 control. The design is modular, compact, lightweight, and low power to accommodate operation in airborne and/or remote environments. The complete package fits in a standard 4-inch optical mount and can be configured to accommodate mirrors with up to 512 actuator channels.



- Standard 25 mm / 37 actuator MDM
- Al or HR coatings
- Discrete component and *Supertex* (SX) HV amplifier Drivers
- Up to 40 Channels on PC P-port
High Bandwidth
Digital Interface
SX Stackable to 1024 channels
Lightweight, Low Power

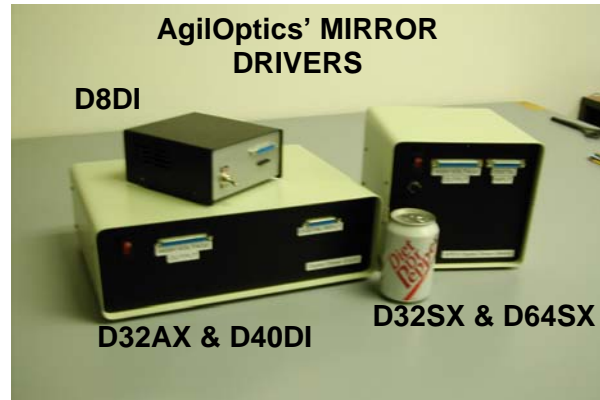
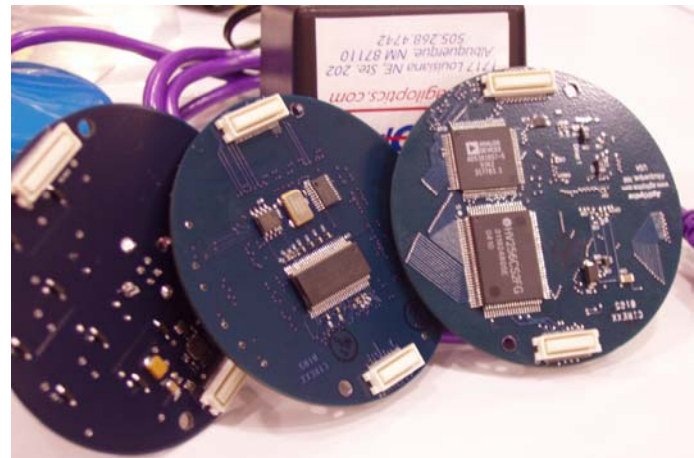


Figure 2. AgilOptics standard commercial MDM mirror designs



- Faster USB Connection
- 3 Stackable PC Boards
- Modules of 64 channels
- <3w Total Power (64 channels)
- 75g total Weight



- 3.5" Diameter
- 32-ch Supertex HV Amps
- 4kHz Operation over USB 2.0
- 512 Channels, Max

Figure 3. Recently developed MDM driver using USB 2.0 communications interface.

3.0 ELECTROSTATIC MEMBRANE DM THEORY

The static and dynamic behavior of a membrane subjected to an electrostatic force is described by the theory given in References 1 through 3. In addition, Reference 3 provides experimental measurements of MDM performance that verify much of the theory. The most basic theory is summarized here for completeness. For more details, see these References and Reference 4 for a description of our MDM modeling approach based on this theory.

Membrane mirror steady-state deflection is governed by the Poisson equation given by:¹⁻³

$$\nabla^2 Z = -\left(\frac{F(r)}{T}\right) \quad (1)$$

where: Z is membrane deflection, T is membrane tension per unit length, and F is force on the membrane at a point r . For an electrostatic MDM, the force of an actuator pad with applied voltage on the membrane is given by:^{1,3}

$$F_k = \frac{\epsilon Area_k V_k^2}{2D_{sep}^2} \quad (2)$$

where:

F_k - force on membrane due to actuator pad k

ϵ - permittivity of free space

$Area_k$ - area of actuator pad k

V - voltage applied to pad k

D_{sep} - membrane to pad array separation

Reference 3 provides an analytical solution to equation (1) that describes the steady-state membrane deflection for an actuator in the center of the membrane. Reference 4 provides a more generalized empirical solution for an actuator located at any position beneath the membrane. However, the complex interaction of membrane stress and applied force during actuation requires the use of Finite Element Analysis (FEA) to obtain accurate MDM modeling results.

The fundamental frequency of a membrane DM is important for determining the temporal response of a given mirror design. Neglecting friction and air damping the fundamental frequency of a membrane of diameter D , tension/meter T , and mass/area, σ , is given by:¹⁻³

$$f_0 = \frac{2.4}{\pi D} \sqrt{T/\sigma} \quad (3)$$

Equation (3) is valid for small membrane deflections in a vacuum. We present measurements in Section 5.0 indicating that large membrane deflections produce fundamental frequencies much less than those given by this equation.

4.0 MEMS DM SYSTEMS

AgilOptics develops MDM control software for both open and closed-loop operation. The Graphical User Interfaces (GUIs) for our open-loop High Voltage Digital Driver (HVDD) and closed-loop Clarifi-2D systems are shown in Figure 4. HVDD provides for manual and open-loop mirror control for mirror testing and for mirror applications with predetermined mirror response requirements. HVDD operates with all of the mirrors and drivers offered by AgilOptics. Clarifi-2D uses metric optimization dithering techniques to perform wavefront control by improving appropriate metrics based on far field or image intensity measurements. The Clarifi-2D GUI shows the CCD measurement frame, current actuator voltages, and metric value convergence history using the Zernike dither algorithm. Other Clarifi-2D processing algorithms are available using the window tabs on the left. Manual actuator voltage control is available using displayed buttons and the actuator pattern display or using functions under the Voltage Control tab. Metrics are selected and tested using functions under the Feedback tab. Several different versions of Clarifi are available for different closed-loop control scenarios. Details of these systems are given below.

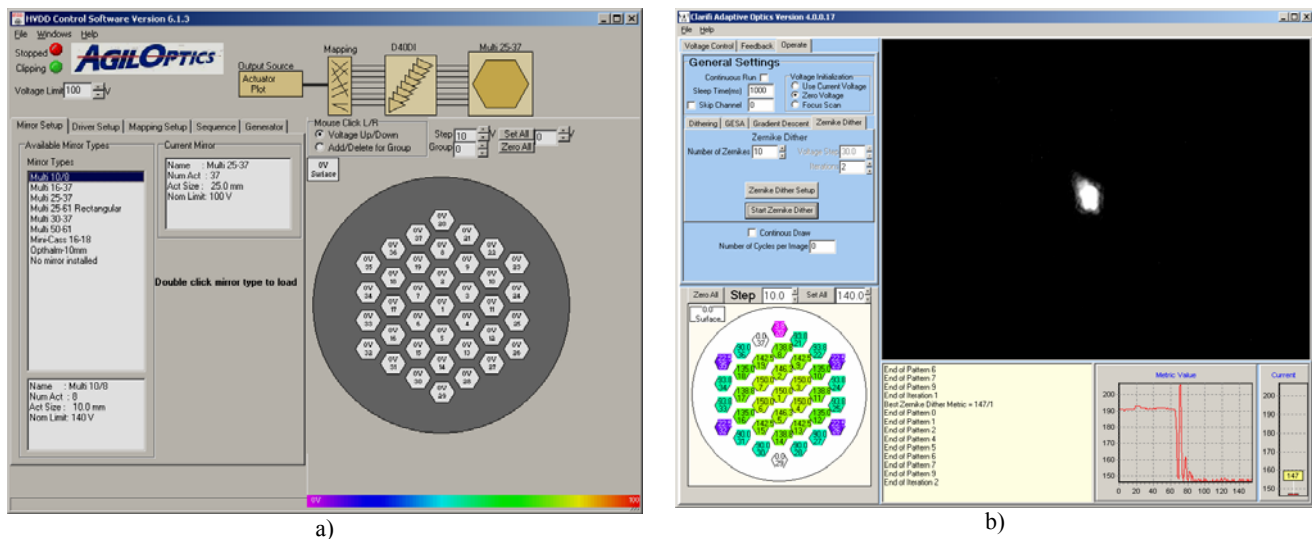


Figure 4. AgilOptics developed GUI for a) open loop (HVDD) and b) closed loop (Clarifi-2D) MDM control

AgilOptics offers three levels of closed-loop adaptive optics systems using both metric optimization and WaveFront Sensor (WFS) feedback. All of the closed loop systems are identified by the trade name “Clarifi.” Clarifi-1D uses metric optimization techniques and a single point metric measurement to improve 1-D system performance. Optimizing the amount of laser energy coupled into a fiber is a typical application for Clarifi-1D. Clarifi-1D operates at 60-100 cycles/sec depending on the system and algorithm used. The metric optimization algorithms available include Guided Evolution Simulated Annealing (GESA), Stochastic Parallel Gradient Descent (SPGD)¹¹, and actuator dithering. Clarifi-2D uses metrics calculated from 2-D CCD measurements. Available metrics include peak or average intensity, spot size, and beam shape for far-field measurements and image sharpness for imaging applications. In addition to the Clarifi-1D optimization algorithms, Clarifi-2D also has Zernike and Fourier dithering algorithms. Clarifi-2D operates at 15-20 cycles/sec limited primarily by a 30 frame/sec frame-grabber. Clarifi-3D uses WFS measurements to minimize the RMS WaveFront Error (WFE) in an optical beam wavefront profile. An initial calibration procedure based on Zernike polynomial terms is used to calculate a control matrix for minimizing the RMS WFE in the least-squares sense. Clarifi-3D wavefront sensing is accomplished using a Hartmann WFS (HWFS) developed by Spiricon, Inc. and a 30 frame/sec frame-grabber that limits temporal closed-loop performance to about 3-cycles/sec. AgilOptics is currently developing an embedded system named ClariFast to provide improved temporal bandwidth using a high-speed camera for Hartmann wavefront sensing and a dedicated processor for closed-loop control.

The Clarifi-3D GUI screen shot shown in Figure 5 a) illustrates the diagnostics available for closed-loop operation with a HWFS. The diagnostics include displays of wavefront slopes, reconstructed wavefront, actuator voltages, Zernike decomposition, and Zernike convergence history. The software can be commanded to minimize WFE or to optimize production of a particular Zernike aberration by the mirror using techniques similar to other closed-loop MDM system investigations.^{14,15} System calibration is controlled by the checklist on the left side of Figure 5 a). The calibration procedure results in mirror influence functions and a control matrix for closed-loop processing.

The embedded Clarifi system (ClariFast) is designed to operate with AgilOptics’ Unifi mirror driver and a high speed camera developed by Southern Vision Systems, Inc. (SVSI). The conceptual system layout is shown in Figure 5 b). Both camera and mirror systems communicate with a dedicated processor controller over USB 2.0 links. The processor is controlled remotely using an Ethernet interface to a PC running a system setup and diagnostic GUI. With current software and planned upgrades we expect to be able to operate the system at 50 closed-loop cycles/second using the current 300-MHz Pentium III processor. Using a faster processor for this system will further improve closed-loop performance.

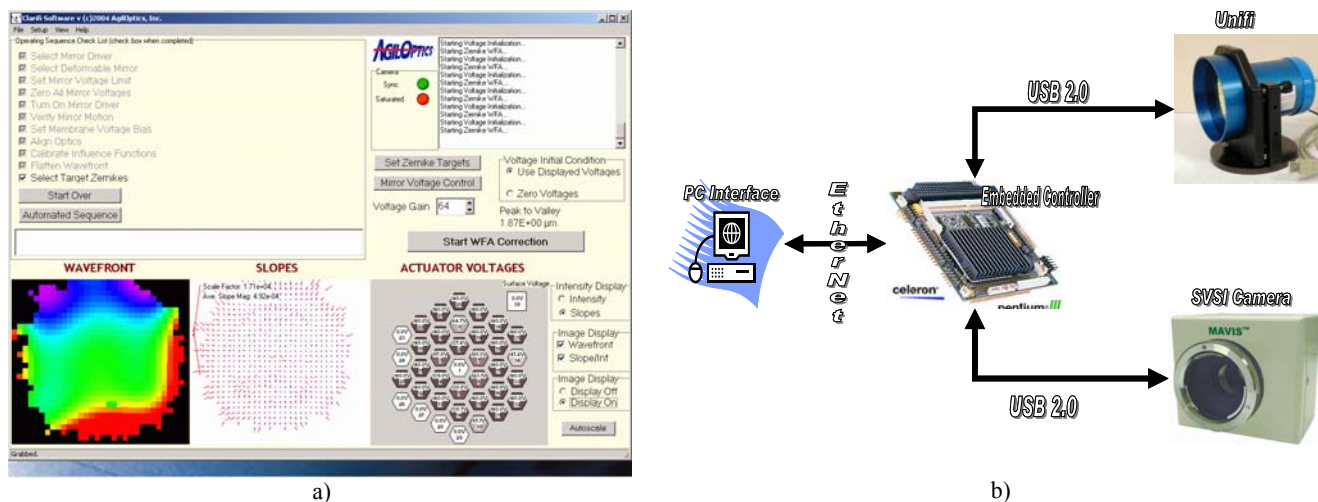
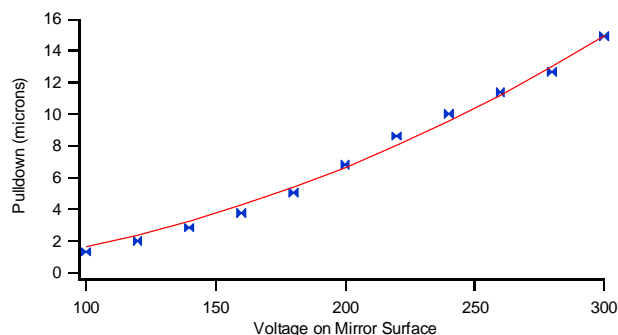


Figure 5. a) GUI for Clarifi-3D b) conceptual design of embedded Clarifi system

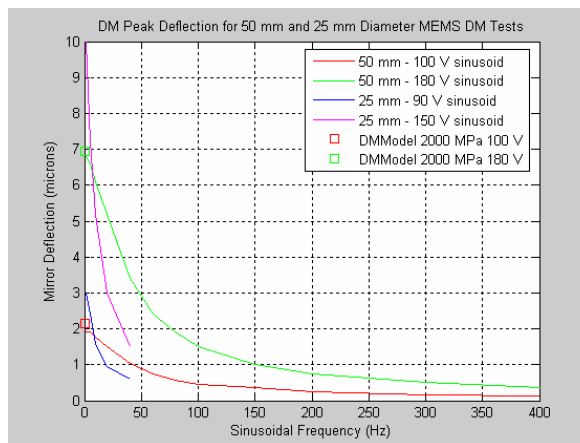
5.0 MEMS DM CHARACTERIZATION

AgilOptics has manufactured operational mirrors as large as 75 mm in diameter. One of the challenges in MDM fabrication is to produce mirrors with good static flatness. This is easily accomplished for smaller mirrors (16 and 25 mm), but more difficult for larger 50 and 75 mm mirrors. Maximizing membrane throw provides opportunity for correcting higher magnitude aberrations. MDM throws approaching membrane snap-down are possible with AgilOptics' Anti-SnapDown (ASD) fabrication process. Measurements of MDM temporal response show that air damping significantly reduces the magnitude of aberrations correctable at higher operating frequencies. Measurements in a vacuum environment allow for analysis of MDM resonance behavior.

The curve in Figure 6 a) shows the maximum throw of a 25 mm MDM with a 46-micron gap to be about 15 microns at 300 volts actuation. This is very close to the snap-down voltage for this mirror. Throws of this magnitude can now be obtained without fear of mirror rupture due to snap-down. Electrostatic snap-down generally occurs when the membrane pull-down surpasses 1/3 of the static membrane to actuator pad array gap. AgilOptics' ASD technology prevents rupture if snapdown occurs. Figure 6 b) shows measurements of 25 and 50 mm MDM responses to large-signal sinusoidal voltages of varying frequency on all actuators. Air damping severely limits the response at higher frequencies, particularly for the 25 mm MDM. Membrane diameter and effective membrane tension have significant effects on membrane deflection. Small signal deflections about a bias voltage should provide improved deflection measurements at higher frequencies.



a)



b)

Figure 6. a) MDM throw can approach the snap-down limit with AgilOptics' Anti-Snap-Down (ASD) technology b) full membrane throw is limited in temporal frequency by air damping and varies with membrane diameter and tension.

Figure 7 illustrates MDM spatial correction capabilities. Figure 7 a) and b) show the production of two Zernike term distributions using a MDM and compare them with results from electrostatic modeling. Comparison of modeling and measurement has shown that the theory is well understood and accurately represents many MDM characteristics.^{12,13} Figure 7 c) and d) compares the performance of 37 and 632 actuator MDMs in correcting for individual Zernike aberrations. The bar graphs show the residual RMS phase error and corrected Strehl Intensity provided by each device in compensating for 0.5 micron RMS Zernike aberrations for the Zernike terms numbered 5 through 22 (5th order spherical aberration). Performance is significantly improved for all of the Zernike terms by using a large number of actuator pads. Residual error is close to $\lambda/20$ RMS (red line) for the 3rd order terms when 632 actuators are used. Larger residual errors are evident for the higher order Zernike terms, indicating more difficulty in fitting the mirror surface to these aberrations.

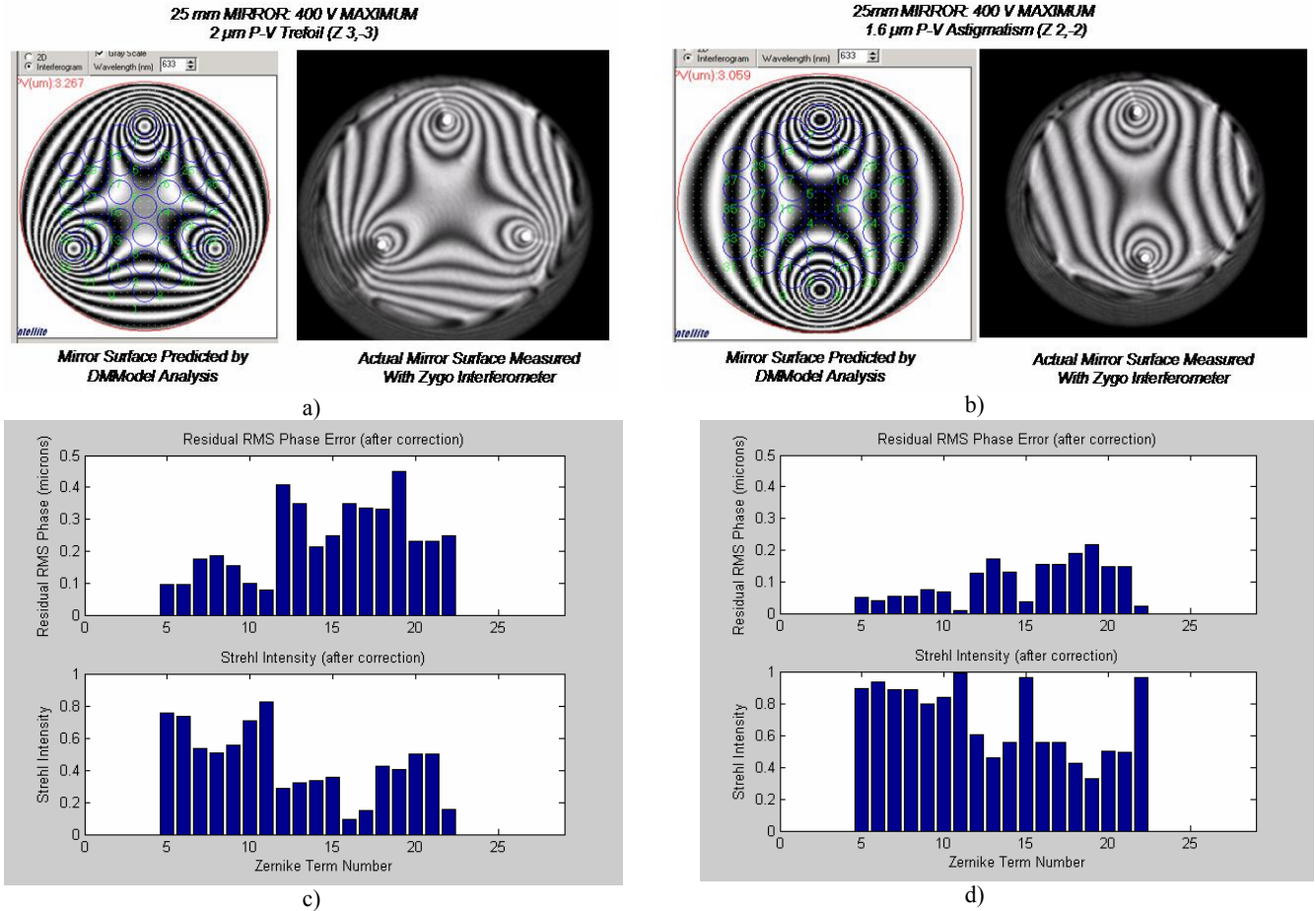
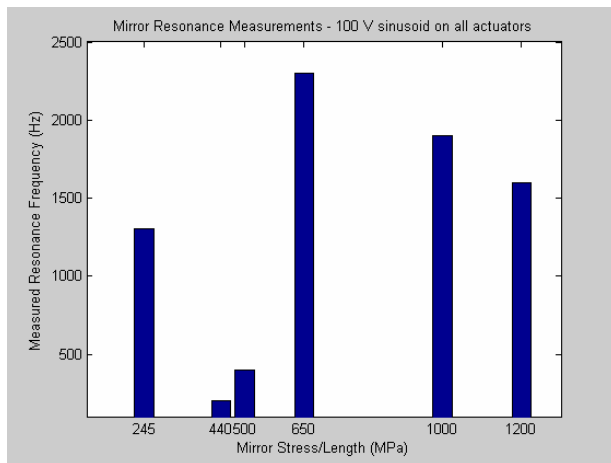
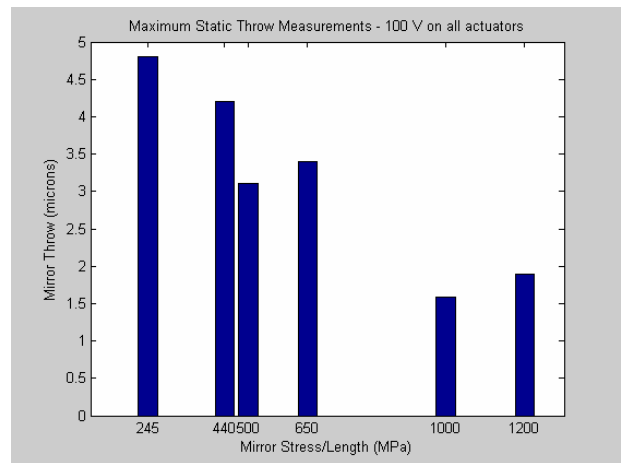


Figure 7. a) Simulated and measured Zernike Trefoil, b) Simulated and measured Zernike astigmatism, c) 37-actuator MDM correction of 0.5 microns RMS Zernike aberrations, d) 632-actuator MDM correction of 0.5 microns RMS Zernike aberrations.

Resonance frequencies were measured for several mirrors with different membrane stress properties. The measurements were made by applying a 100 V sinusoidal voltage to all MDM actuators to induce significant membrane throw. The throw obtained statically for each mirror at 100 V is given in the bar chart in Figure 8 b). The effective membrane stress was inferred using measured membrane-to-actuator pad gap data and analytical modeling of each mirror. The resonance frequencies obtained for each mirror are given in the bar-chart of Figure 8 a) plotted at the inferred stress level for each mirror. Resonance was easily measured using a Laser Doppler Vibrometer (LDV) by observing MDM response to sinusoidal voltages on all actuator pads. The resonance behavior varied significantly and with membrane stress and was much less than that predicted by membrane theory. We believe that the theory predictions are more appropriate for small-signal localized driving frequencies rather than the large signal applied here to all actuator pads. The oscilloscope traces shown in Figure 9 illustrate the onset of resonance observed in making the LDV measurements.

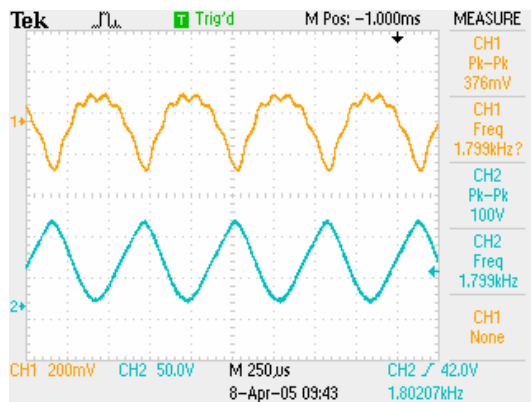


a)

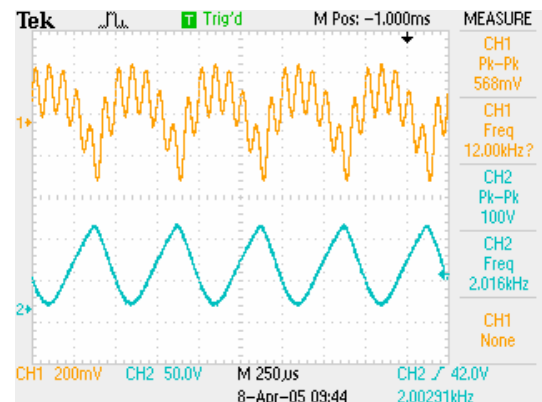


b)

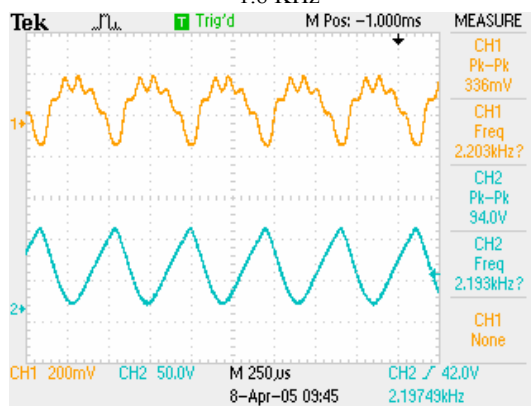
Figure 8. a) Large throw resonance measured in vacuum for mirrors with different membrane stress b) Mirror throw variation with membrane stress using a 100 V sinusoidal driving function



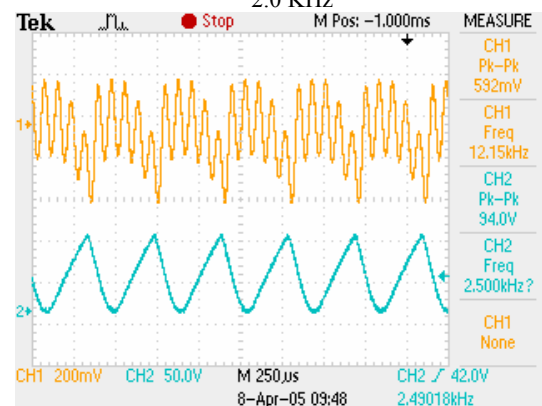
1.8 KHz



2.0 KHz



2.2 KHz



2.5 KHz

Figure 9. Electrostatic MDM near resonance behavior with a large amplitude driving frequency. Resonance occurs at 2.4 KHz.

The curves in Figure 10 illustrate frequency response measurements for two mirrors with different characteristics and under different operating conditions. The plot in Figure 10 a) shows mirror response at 1 torr, 7.5 torr, 15 torr, and at atmospheric pressure. Resonance was observed at 400 Hz when operating at 1 torr with large mirror throw. Resonance increased to about 500 Hz at 7.5 and 15 torr with reduced response due to increased damping. Increased damping at atmospheric pressure further reduced the response and eliminated the resonance behavior. The plot shown in Figure 10

b) indicates that good mirror response can be obtained at higher frequencies at atmospheric pressure if air is vented from between the membrane and pad array gap. Reducing gas density with venting (using helium) further improves results at all frequencies. Membrane deflection as high as 0.728-microns was obtained at 1 KHz operation in atmosphere by applying a 225 V (P-V) sinusoid.

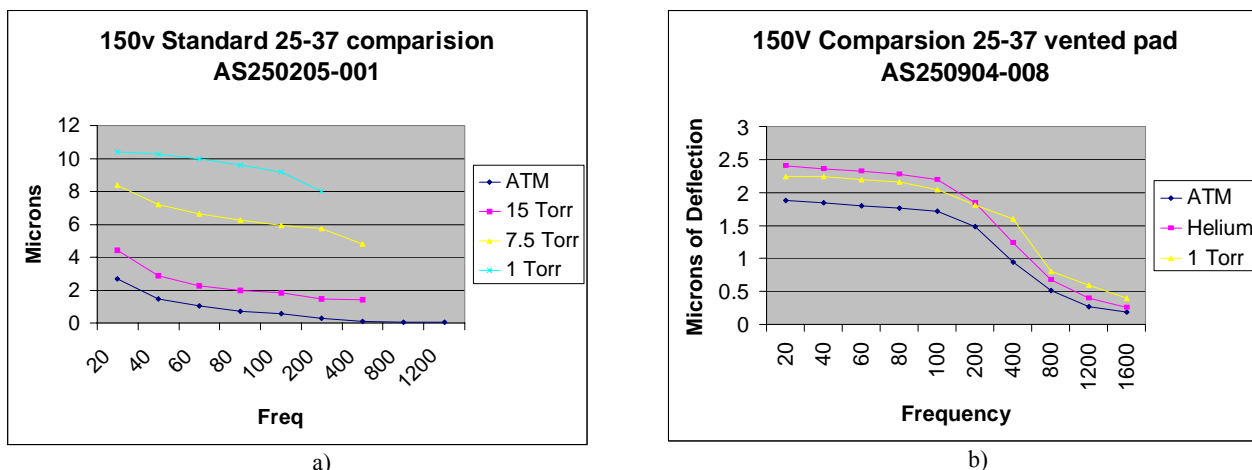


Figure 10. a) Large signal resonance occurs at low frequencies b) air damping and resonance effects are greatly reduced with pad array venting.

In summary, the frequency response measurements presented were only obtained for large voltage pull-down of the membrane using the entire actuator pad array. The measured resonance frequencies for this case were much lower than theory predicts for localized small signal variations. Air-damping severely limits MDM large-signal throw at high frequencies. Additional measurements have shown that high frequency throw is improved with higher tension membranes, larger membrane to pad array spacing, and pad array air venting. Operating in a partial vacuum or in lower gas density also improves throw and frequency response.

5.0 MEMS DM APPLICATIONS

AgilOptics has conducted application demonstrations using HVDD, Clarifi-1D, 2D, and 3D and using custom built MDM driver electronics. Clarifi-1D has been used to demonstrate optimization of laser coupling into a 4-micron single mode fiber. As shown in Figure 11 a), the laser beam was expanded, reflected off the MDM and focused into a fiber end. The energy entering the fiber was detected by a photodiode and passed through an A/D converter to provide Clarifi-1D with an energy-metric for optimization. The total coupled energy was increased by 225 to 750% over best manual alignment by using Clarifi-1D in 5 separate trials. Real-time display of the metric (shown in Figure 11 b)) provides feedback on the optimization process.

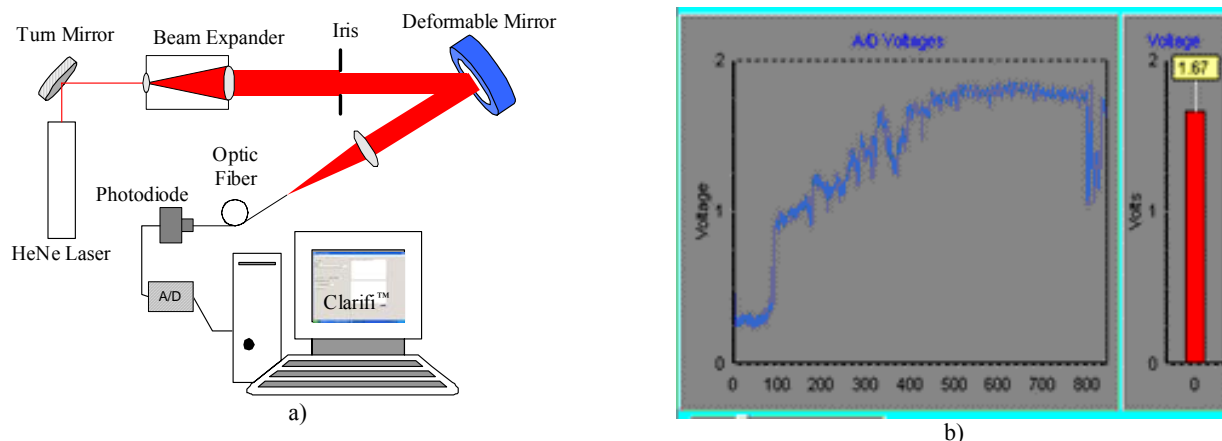


Figure 11. a) Large signal resonance occurs at low frequencies b) air damping and resonance effects are greatly reduced with pad array venting.

Figure 12 shows the basic Clarifi-2D and Clarifi-3D setup for closed loop wavefront control. Clarifi-3D uses a wavefront sensor rather than the video camera and focusing lens used for Clarifi-2D far-field optimization. Clarifi-3D closed-loop control is similar to systems presented in References 14 and 15. Laser beam shaping was demonstrated using HVDD and Clarifi-2D using the slightly modified setup shown in Figure 13. HVDD was used to manually redistribute the beam intensity and Clarifi-2D was used to correct the phase of the resulting beam. The results of the laser beam shaping demonstration are shown in Figure 14. The initial Gaussian beam intensity (Figure 14 a)) was manually redistributed using HVDD to form a square annular beam (Figure 14 b)) in the near field. The resulting far field intensity distribution, indicating severe phase errors in the redistributed beam, is shown in Figure 14 c). After phase error correction using Clarifi-2D with closed-loop metric optimization, the far field assumes the focused, point-like distribution shown in Figure 14 d).

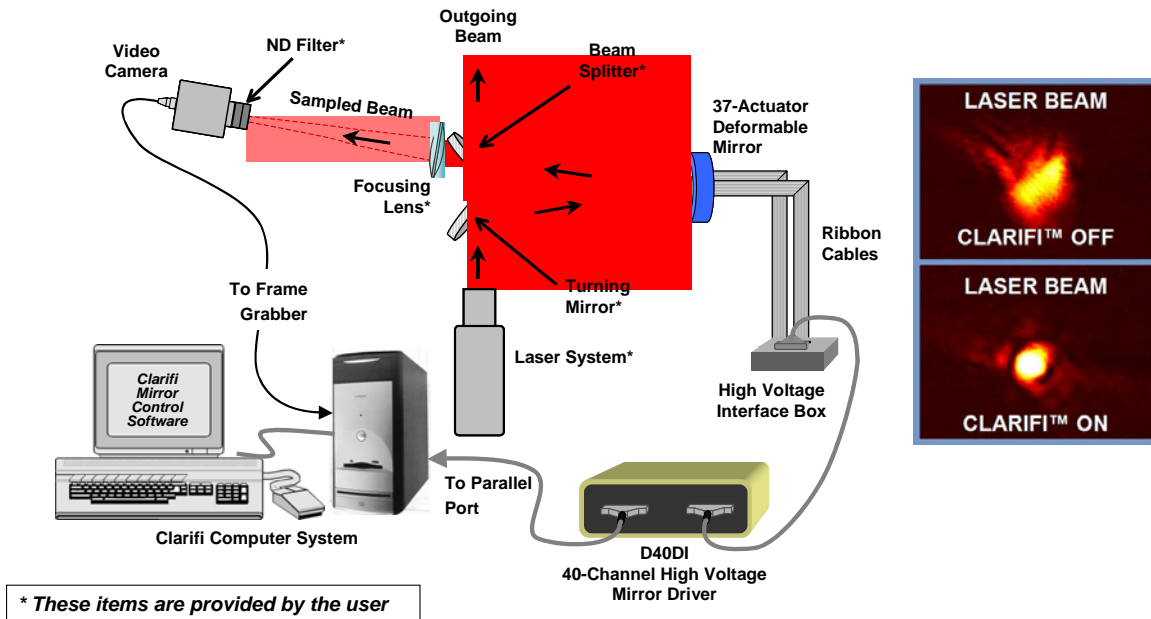


Figure 12. Clarifi-2D system configured to optimize far field spot metrics. Clarifi-3D is configured in a similar manner with the CCD and focusing lens replaced by a wavefront sensor

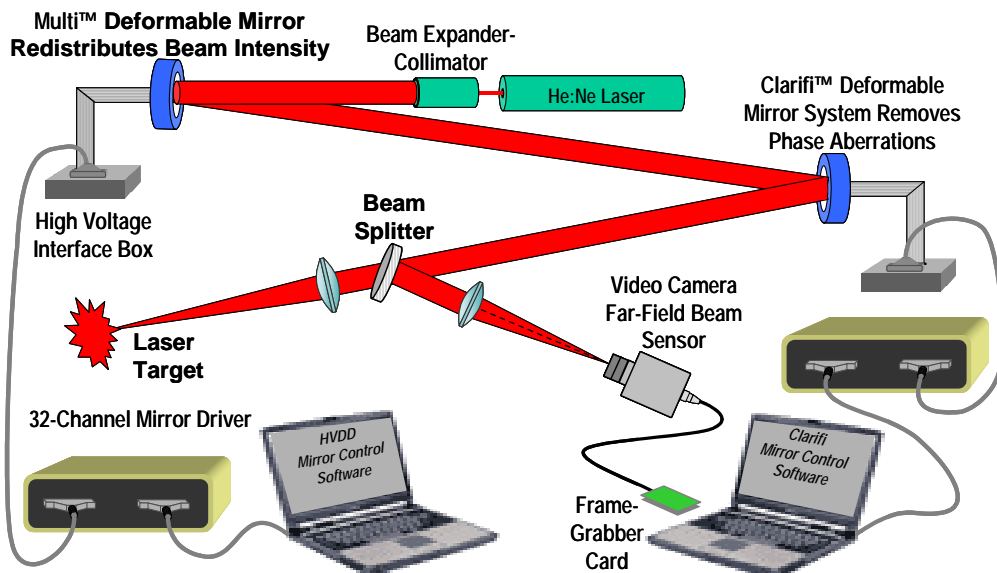


Figure 13. Clarifi-2D and HVDD setup to demonstrate beam shaping.

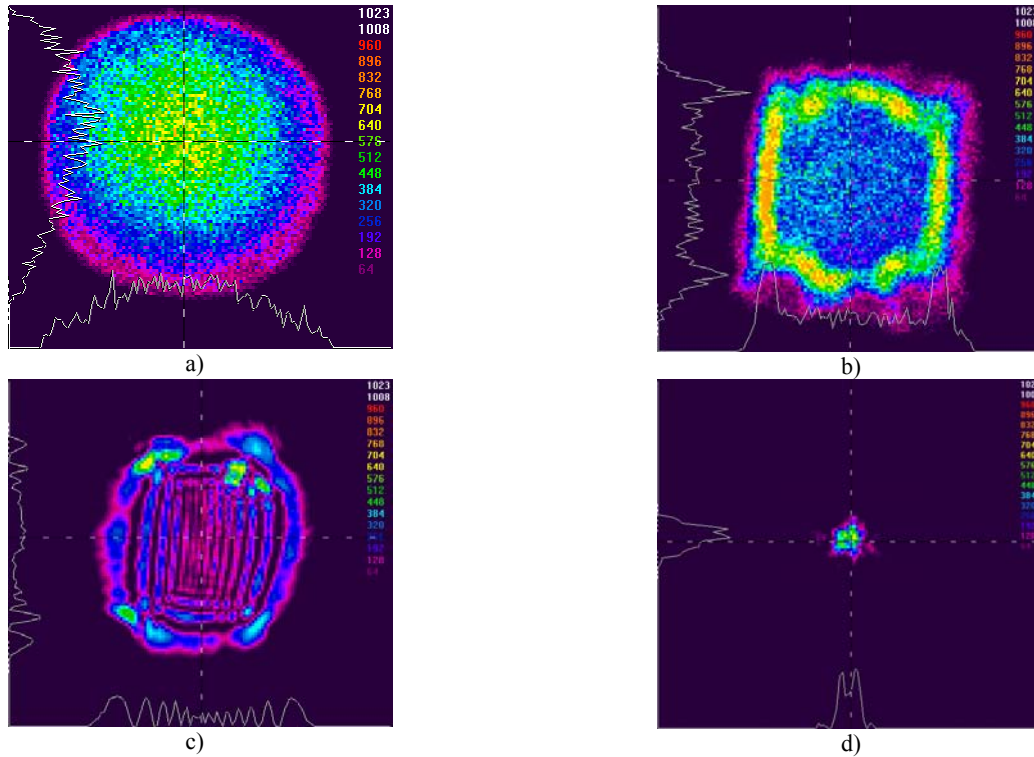


Figure 14. Results from beam shaping demonstration. a) initial near field Gaussian beam b) near field square annulus after intensity redistribution using HVDD c) far field of square annulus before phase correction d) far field after phase correction with Clarifi-2D

Figure 15 depicts a possible high-power Intra-Cavity Adaptive Optics (ICAO) application demonstration using an MDM with a High Reflectivity (HR) coating. AgilOptics has demonstrated HR-coated MDM operation for 15 and 60-second intervals with up to 40 kW/cm^2 energy density on the mirror, without damage (for 1315 and 1064 nm wavelengths, respectively). Additional high power demonstrations have shown that cooling of the mirror back-structure will be required for extended operation. We are currently pursuing options for cooling our MDM designs.

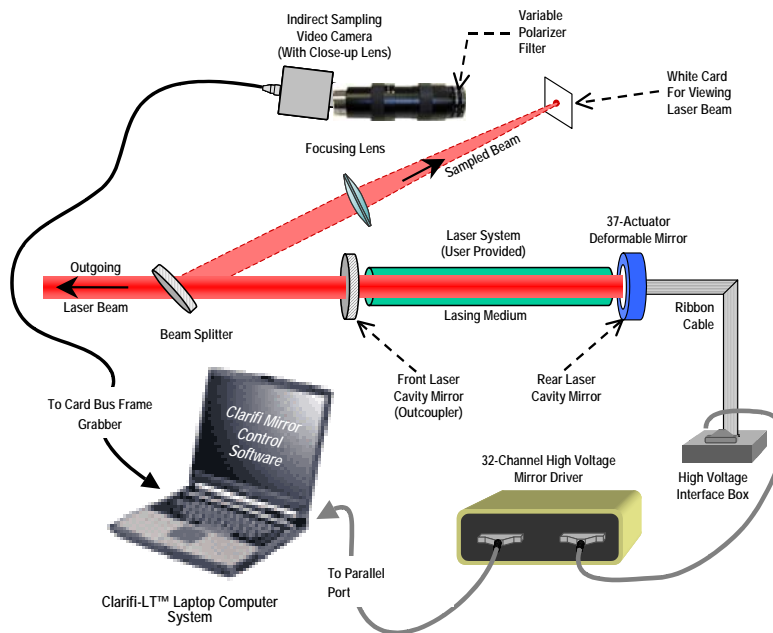


Figure 15. Clarifi-2D setup to demonstrate Intra-Cavity Adaptive Optics.

In cooperation with the University of Notre Dame, AgilOptics has demonstrated correction of a regularized aero-optics flow field using a MDM. Acoustic forcing on a flow field can cause the optical aberration produced by the turbulent flow to become periodic and predictable.¹⁶ This allows for open-loop correction of the disturbance using a DM when the DM actuator commands are properly phased with the regularized flow disturbance. The approach used is depicted in Figure 16. The experiment used a heated jet and a woofer to produce an aberration at 240 Hz with a peak-valley magnitude of about 0.2 microns. Since the heated jet disturbance was primarily one dimensional, AgilOptics developed a mirror with a linear pad array for correction (shown in Figure 17). AgilOptics also developed custom electronics to update the MDM actuator commands at a 3.6 KHz rate to ensure correction of the 240-Hz disturbance.

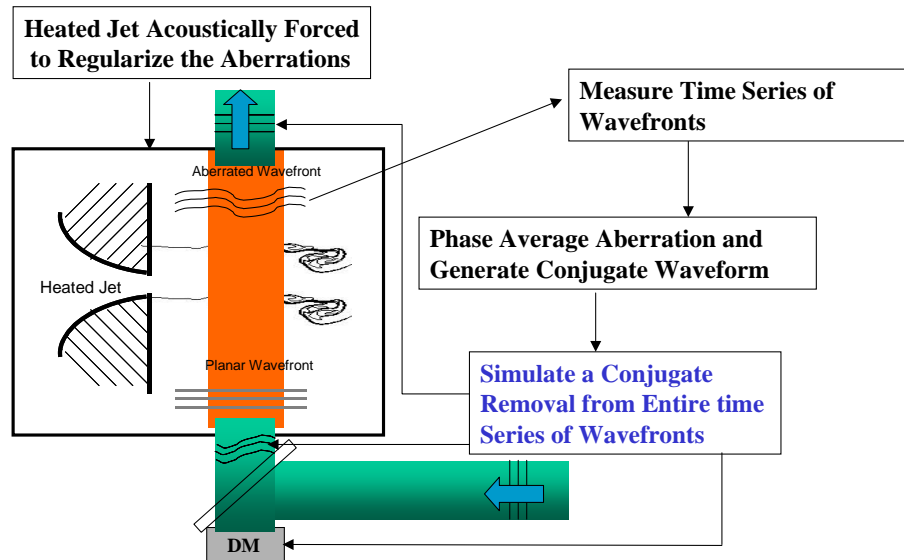


Figure 16. Conceptual diagram illustrating forced regularization of aero-optics flow and approach for open-loop correction with a DM

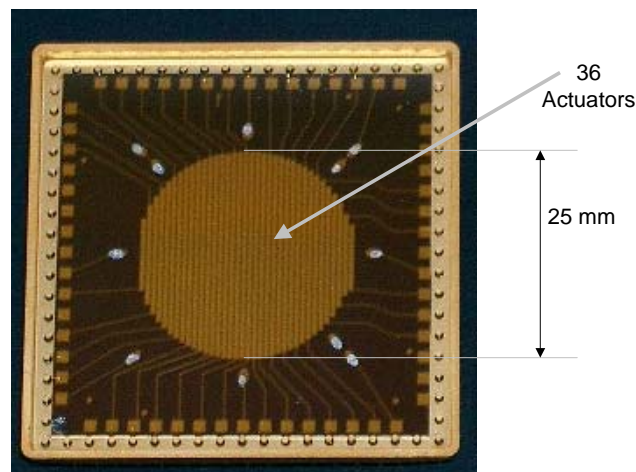


Figure 17. Linear actuator mirror (pad array shown) developed for aero-optics compensation demonstration

One cycle of the 240 Hz signal aberration is shown in Figure 18 a). The vertical axis represents the distance across the mirror and the horizontal axis represents the time during a period. The predicted residual correction error for the same period based on physical mirror modeling is shown in Figure 18 b). This corresponds to an average residual RMS phase error of about 0.04 microns and a Strehl Intensity of about 0.9. Prior to performing the experiment, we measured mirror surface displacements as a function of the driving signal over each actuator. Some of these results are presented in Figure 18 c) and d) for mirror surface displacements above actuators 18 and 27, respectively. Except for a time delay

of about 700 microseconds the mirror surface measurements were found to agree quite well with the commanded mirror displacements (the signals shown here are shifted in time for a best match of the desired and measured signals). Mirror voltage commands were determined from mirror influence function modeling and least-squares correction of the spatial distribution of the periodic signal across the mirror for each of 36 time-steps during a signal period.

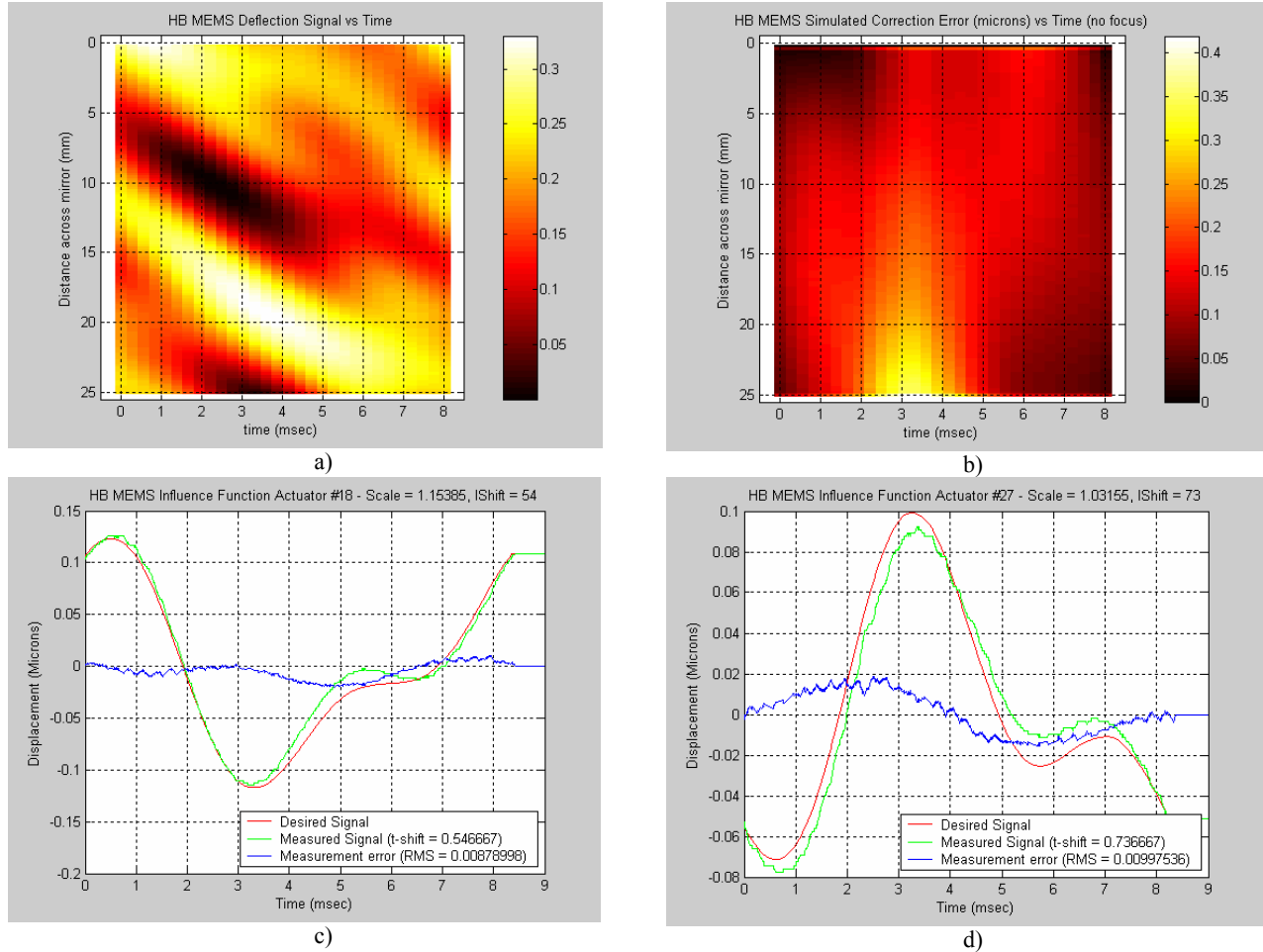


Figure 18. a) one-period of forced regularized aero-optics aberrations b) simulated residual error from correction with linear array MDM c) LDV measurement of mirror response compared to desired signal at actuator 18 d) LDV measurement of mirror response compared to desired signal at actuator 27.

Strehl Intensity calculations, shown in Figure 19, illustrate the improvement obtained in the experiment with MDM AO correction. This was the first time that aero-optics compensation was demonstrated using open-loop DM correction of a flow field regularized with acoustic forcing. The AO system consisted of a 25 mm MDM, a small driver box with high speed electronics (MDM commands at 3.6 KHz), and a laptop computer with software for loading correction signals into the electronics FPGA. Correction has since been demonstrated for the same experiment, using a Xinetics mirror system, with nearly identical results.¹⁶

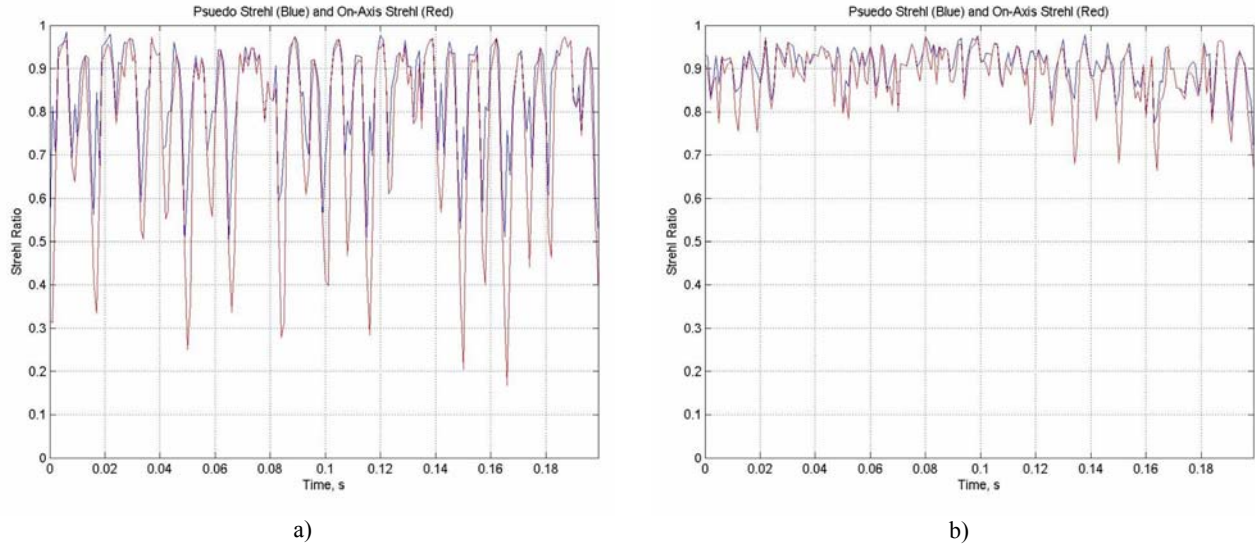


Figure 19. a) Far field strehl due to regularized aero-optics aberration without correction b) Far field strehl with MDM correction.

6.0 SUMMARY AND CONCLUSIONS

AgilOptics develops and markets complete MDM systems including standard and custom MDM designs, driver electronics, and open and closed-loop control software for both commercial and government applications. HVDD software provides complete manual control of MDMs for design and performance evaluation and open-loop control using predetermined mirror response functions. The Clarifi-1D, 2D, and 3D software packages provide closed-loop MDM control, in a PC-based GUI environment, using metric optimization and Hartmann WFS measurements to satisfy different levels of wavefront control requirements. We are currently developing an Embedded Clarifi system that will use a HWFS with a high-speed camera and dedicated processing capabilities to provide higher bandwidth wavefront control using remote PC-based GUI control. We expect this system to provide correction with measurement and control at greater than 50 Hz.

Spatial and temporal characterization results were presented to address MDM membrane flatness, membrane throw, Zernike correction and temporal frequency response. We routinely produce mirrors with flatness to 400 nm P-V and with maximum membrane throw exceeding 10 microns. Frequency response measurements showed that aberration correction in excess of 1-micron P-V is possible at 1 KHz operation with air damping. Large signal mirror response measurements in a vacuum, using 25 mm diameter mirrors, indicate resonance frequencies varying from 300 to 2300 Hz depending largely on the membrane stress of the mirror under test. Additional measurements are required to compare small signal resonance behavior with membrane theory.

MDM applications demonstrated using AgilOptics developed systems were discussed in some detail. The demonstrations included laser beam quality improvement, laser beam shaping, high-power operation for IntraCavity Adaptive Optics (ICAO), and aero-optics regularized flow compensation. The aero-optics MDM experiment presented here was a land-mark accomplishment. This is was the first time that any DM had been used to demonstrate correction of aero-optics turbulence using the regularized flow approach developed at the University of Notre Dame. It is satisfying to say that the first DM to show that this was possible was an MDM.

7.0 ACKNOWLEDGEMENTS

The work required for this manuscript was supported by the Air Force Research Laboratory's Directed-Energy-Directorate, at Kirtland AFB, New Mexico, with funding from the Joint Technology Office (JTO) and the Small Business Innovative Research (SBIR) Office. We would also like to acknowledge Dennis Mansell, President of AgilOptics, for his foresight and leadership in developing this technology and AgilOptics' employees Harvey Packard and Don Owens for their support in developing State-Of-the-Art software and electronics that make these accomplishments in MDM systems possible.

REFERENCES

1. M. Yellin, "Using membrane mirrors in adaptive optics," Proc. SPIE, Vol. 75, (1976).
2. P. M. Morse, Vibration and Sound, McGraw-Hill, (1948).
3. R. P. Grosso and M. Yellin, "The membrane mirror as an adaptive optical element," J. Opt. Soc. A., Vol. 67, No. 3, March 1977.
4. K. Bush, D. German, B. Klemme, A. Marrs, and M. Schoen, "Electrostatic membrane deformable mirror wavefront control systems: design and analysis," Proc. SPIE, Vol. 5553, 28-38, (2004)
5. G. Vdovin and P. M. Sarro, "Flexible mirror micromachined in silicon," App. Opt., Vol. 34, No. 16, 1 June 1995.
6. G. Vdovin, "Optimization-based operation of micromachined deformable mirrors," Proc. SPIE, Vol. 3353, (1998).
7. J. A. Perrault, T. G. Bifano, B. M. Levine, M. N. Horenstein, "Adaptive optic correction using microelectromechanical deformable mirrors," Opt. Eng. 41(3), 561-566 (March 2002).
8. E. J. Fernandez, I Iglesias, P. Artal, "Closed-loop adaptive optics in the human eye," Opt. Let., Vol.26, No.10, May 15, 2001.
9. J. Gonglewski, D. Dayton, S. Browne, S. Restaino, "MEMS adaptive optics: Field demonstration," Proc. SPIE, Vol. 4839, (2003).
10. P. Villoresi, S. Bonora, M. Pascolini, L. Poletto, G. Tondello, C. Vozzi, M. Nisoli, G. Sansone, S. Stagira, and S. DeSilvestri, "Optimization of high-order harmonic generation by adaptive control of a sub-10-fs pulse wave front," Opt. Let., Vol. 29, No. 2, January 15, 2004.
11. M. A. Vorontsov and V. P. Sivokon, "Stochastic parallel-gradient-descent technique for high-resolution wavefront phase-distortion correction," J. Opt. Soc. Am. A, Vol. 15, No. 10, October 1998.
12. L. Zhu, P. Sun, D. Bartsch, W. R. Freeman, Y. Fainman, "Wavefront generation of Zernike polynomial modes with a micromachined membrane deformable mirror," App. Opt., Vol. 38, No. 28, 1 October 1999.
13. E. J. Fernandez and P. Artal, "Membrane deformable mirror for adaptive optics: performance limits in visual optics," Opt. Exp., Vol. 11, No. 9, 5 May 2003.
14. L. Zhu, P. Sun, D. Bartsch, W. Freeman, and Y. Fainman, "Adaptive control of a micromachined continuous-membrane deformable mirror for aberration compensation," App. Opt., Vol. 38, No. 1, 1 January 1999.
15. C. Paterson, I. Munro, and J. C. Dainty, "A low cost adaptive optics system using a membrane mirror," Opt. Exp., Vol. 6, No. 9, 24 April 2000.
16. D. A. Duffin, "Feed-Forward Adaptive-Optic Correction of Aero-Optical Aberrations Caused by a Two-Dimensional Heated Jet," Proc. AIAA, Vol. 4776, (June 2005).